Two-loop virtual amplitudes for $q\bar{q} \to t\bar{t}H$ production (the N_f part)

Vitaly Magerya[*]

Institute for Theoretical Physics, Karlsruhe Institute of Technology,
Wolfgang-Gaede-Str. 1, Geb. 30.23, 76131 Karlsruhe, Germany

E-mail: vitalii.maheria@kit.edu

In this article we briefly review the recent calculation of the part of two-loop virtual amplitudes for $q\bar{q} \to t\bar{t}H$ production proportional to the number of light and/or heavy quark flavours, the methods and tools employed (integral evaluation via sector decomposition with pySecDec, and IBP reduction with Rational Tracer), with an eye towards the full NNLO calculation.

---

[*]Speaker

1. Introduction

The production of a Higgs boson (H) in association with a top-quark pair ($t\bar{t}$) at LHC is experimentally interesting because it provides direct access to the top–Higgs Yukawa coupling. The first observation of such events have been reported on by both ATLAS and CMS collaborations in 2018 [1, 2], with earlier evidence reported in [3–5] and more analyses being done since then [6–10]. The latest results are based on the data from 2015–2018 (i.e. LHC Run II); here are some of them:

	$\sigma_{t\bar{t}H}$, Experiment/$\sigma_{t\bar{t}H,\text{Standard Model}}$		$\mathcal{L}$	H decay channels
ATLAS '18 [1]	1.32	$^{+0.18}_{-0.18}$(stat) $^{+0.21}_{-0.19}$(syst)	79.8 fb^{-1}	$\gamma\gamma, bb, WW, ZZ$
ATLAS '20 [6]	1.43	$^{+0.33}_{-0.31}$(stat) $^{+0.21}_{-0.15}$(syst)	139 fb^{-1}	$\gamma\gamma$
CMS '20 [8]	1.38	$^{+0.29}_{-0.27}$(stat) $^{+0.21}_{-0.11}$(syst)	137 fb^{-1}	$\gamma\gamma$
CMS '20 [9]	0.92	$^{+0.19}_{-0.19}$(stat) $^{+0.17}_{-0.13}$(syst)	137 fb^{-1}	$WW, \tau\tau, ZZ$

These results are not very precise, but already the reported statistical errors are of the same order of magnitude as the theoretical ones. The former ones are largely determined by the available data volume (i.e. the integrated luminosity $\mathcal{L}$), and with the inclusion of the LHC Run III data that is expected to double $\mathcal{L}$, and further inclusion of the LHC-HL data (increasing $\mathcal{L}$ to 3000 fb^{-1}), the statistical error is expected to go down to around 2% [11–13]. The theoretical error, on the other hand, is dominated by uncertainties related to the truncation of the perturbative expansion, with the state of the art being next-to-leading order (NLO) calculations. To improve the theoretical error, a NNLO calculation for the $pp \to t\bar{t}H$ production is needed.

Multiple steps towards a NNLO calculation have been made in the last few years [14–18], but there remains a big missing part: the two-loop virtual amplitudes for $q\bar{q} \to t\bar{t}H$ and $gg \to t\bar{t}H$ with full top-quark mass and Higgs mass dependence. Because the needed quantity is a two-loop five-point amplitude with two masses, for a total of 7 scales, the calculation of it using conventional methods is very resource-intensive—it currently lies at the forefront of what is practically achievable.

In this paper we would like to report on the successful completion of a proof-of-a-concept calculation of the part of the two-loop $q\bar{q} \to t\bar{t}H$ amplitude proportional to the number of light quark flavours and/or heavy quark flavours (the "N_f part"), with full top- and Higgs mass dependence [19]. It is our belief that the method used in this calculation can be extended to the calculation of the remaining non-N_f parts of $q\bar{q} \to t\bar{t}H$, as well as to $gg \to t\bar{t}H$.

2. Calculation method

The object of our interest is the scattering amplitude of the process

$$q(p_q) + \bar{q}(p_{\bar{q}}) \to t(p_t) + \bar{t}(p_{\bar{t}}) + H(p_H), \qquad (1)$$

calculated in QCD with an additional scalar H of mass m_H, n_l light (massless) quarks, and n_h heavy (massive) quarks of mass m_t. This process has a 5-dimensional phase-space. To parameterize it,
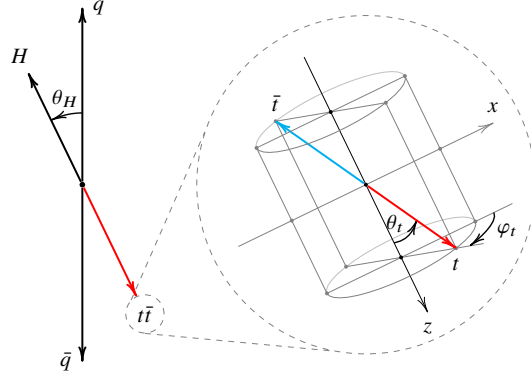
Figure 1: The phase-space parameters. The angles θ_t and φ_t are local to the $t\bar{t}$ rest frame, while θ_H is local to the $t\bar{t}H$ rest frame.

we remap the invariants

$$s = \left(p_q + p_{\bar{q}}\right)^2 \in \left[\,(2m_t + m_H)^2\,;\,\infty\,\right], \tag{2}$$

$$s_{t\bar{t}} = \left(p_t + p_{\bar{t}}\right)^2 \in \left[\,(2m_t)^2\,;\,\left(\sqrt{s} - m_H\right)^2 - (2m_t)^2\,\right], \tag{3}$$

into a hypercube by introducing

$$\beta^2 \equiv \frac{s - s_{min}}{s} \in [0;1], \tag{4}$$

$$\mathrm{frac}_{s_{t\bar{t}}} \equiv \frac{s_{t\bar{t}} - s_{t\bar{t},min}}{s_{t\bar{t},max} - s_{t\bar{t},min}} \in [0;1], \tag{5}$$

and the angles $\theta_H \in [0;\pi]$, $\theta_t \in [0;\pi]$, $\varphi_t \in [0;2\pi]$ as in Figure 1.

We consider the amplitude projected onto Born and expanded in the strong coupling α_s,

$$\langle \mathrm{Amplitude_{tree\text{-}level}} \mid \mathrm{Amplitude} \rangle \equiv \mathcal{A} + \left(\frac{\alpha_s}{2\pi}\right)\mathcal{B} + \left(\frac{\alpha_s}{2\pi}\right)^2 C, \tag{6}$$

where C is our quantity of interest: we shall calculate the N_f part of it, i.e. the part proportional to either n_l or n_h. To do that:

1. We start by generating all diagrams for $q\bar{q} \to t\bar{t}H$ at two loops using QGRAF [20]. There is a total of 702 of them, but only 249 contribute to the N_f part.

2. We insert the Feynman rules using ALIBRARY [21], sum over the spinor and color tensors with FORM [22] and COLOR.H [23]. We get around 90000 scalar integrals contributing to 15 symbolic structures (i.e. gauge-invariant color and flavour structures): $\{n_h|n_l\}\,C_A C_F N_c$, $\{n_h|n_l\}\,C_F^2 N_c$, $\{n_h|n_l\}\,d_{33}$, $\{n_h|n_l\}^2\,C_F N_c$; $C_A^2 C_F N_c$, $C_A C_F^2 N_c$, $C_F^3 N_c$, $C_A d_{33}$, $C_F d_{33}$, d_{44}. Only the first 9 of these are proportional to n_l or n_h; for them only 20000 integrals need to be considered.

3. We resolve integral symmetries using FEYNSON [24, Chapter 4] and sort integrals into families (topologies). We find 89 families, with only 44 contributing to the N_f part, and out of them

only 28 are unique up to permutation of external legs. Here are some of the more complicated integral families:
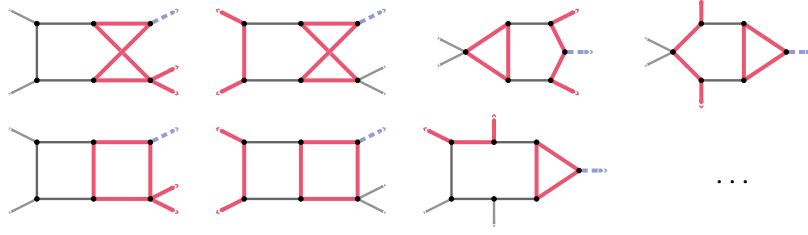
(The thick red lines correspond to massive top quarks, dashed blue legs to the radiated Higgs).

4. We use KIRA [25, 26] to figure out the master integral count in each sector. There are 3005 master integrals in total, with only 831 relevant to the N_f part. We see up to 13 master integrals per sector, but only up to 8 in the N_f part.

5. We optimize the selection of master integrals by considering integrals with raised denominator powers and shifted dimensions, as will be described in Section 2.1.

6. With the chosen master integrals we generate the needed IBP relations with KIRA and dimensional recurrence relations with ALIBRARY, and precompute the IBP solution using Rational Tracer (RATRACER) [27] by constructing a *trace* of the solution. Note that we do not try to solve the full set of equations symbolically, as that is prohibitively complex.

7. We generate and precompile a pySECDEC integration library for the amplitudes; we define each symbolic structure as a separate weighted sum of the master integrals. Because the weights in these sums are to be determined via the solution of the IBP relations, at this stage we only supply pySECDEC with the information about the poles of these coefficient; the actual values will be substituted at a later stage.

8. For each phase-space point of interest we:

   (a) Solve the combined set of IBP and dimensional recurrence relations using the precomputed RATRACER trace. This takes around 2 CPU-minutes.

   (b) Plug in the IBP coefficients into the pySECDEC integration library, and run it (on a GPU) to get the raw amplitude values. This takes from 5 minutes in the bulk of the phase-space to arbitrary large time near the boundaries (e.g. in the high-energy region).

   (c) Combine the 2-loop amplitude with the 1-loop and the tree-level ones to perform renormalization and infrared pole subtraction as described in [28, 29].

   (d) Save the obtained result.

There are three key elements here: choosing the master integrals, solving the IBP relations with RATRACER, and evaluating the integrals with pySECDEC. Let us describe all three in more detail.
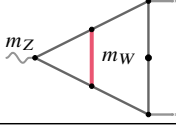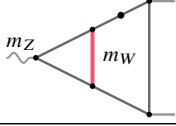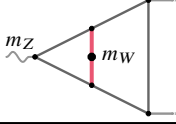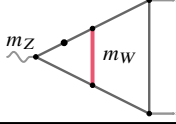
Integral	Orders in ε	Time	Integral	Orders in ε	Time
	$\varepsilon^{-2} \dots \varepsilon^0$	>2h		$\varepsilon^{-2} \dots \varepsilon^0$	20m
	$\varepsilon^{-2} \dots \varepsilon^0$	1m		$\varepsilon^{-3} \dots \varepsilon^0$	27s

Table 1: The time needed to integrate the depicted integrals to 3 digits of precision on an NVidia A100 GPU with pySECDEC 1.5.3.

2.1 Choosing the master integrals

The choice of master integrals greatly affect both the time it takes to solve IBP equations and the time it takes to evaluate the resulting amplitudes numerically. This is why we spend extra effort on it. We choose a basis that:

- is quasi-finite [30];

- is *d*-factorizing [31, 32];

- results in IBP coefficients with small polynomials;

- avoids ε poles in the coefficients of top-level sectors;

- avoids ε poles in the differential equation matrix for the master integrals;

- is fast to evaluate with pySECDEC.

Satisfying all of these conditions simultaneously is not generally possible; instead we make sure the first two are always satisfied, and approach the rest heuristically by trying many different basis choices. In particular, we consider integrals with denominator power raised by up to 6, and dimensionally shifted integrals in $d = 6 - 2\varepsilon$ and $d = 8 - 2\varepsilon$.

As an illustration of the importance of optimizing the master integral choice, consider the task of integrating the integrals in Table 1 to 3 digits of precision: the four integrals differ only in the location of the dot (i.e. which of the denominator is raised to power 2), but the runtime differs by a factor of 200.

2.2 Solving IBP equation with Rational Tracer

The standard methods of solving IBP equations nowadays is the combination of the Laporta algorithm [33] with finite field rational function reconstruction methods [34, 35]. In such an approach one repeatedly solves the system of IBP equations (by Gaussian elimination) while using modular arithmetic and having all variables set to numbers modulo a large (usually 63-bit) prime number. Once the system is solved enough times, it is possible to reconstruct the IBP coefficients as rational functions of the input variables. Many modern IBP solvers, such as KIRA+FIREFLY [36, 37], FIRE6 [38], FINITEFLOW [39], CARAVEL [40], etc, use this method either by default or as an option.

In [27] it was noticed that there is an inefficiency in the common approach to modular Gaussian elimination: a lot of time is wasted on overhead of data management, and not on performing modular arithmetic. A solution was proposed: solve the system once, record each arithmetic operation performed during the elimination forming *an execution trace* (or simply *a trace*), and *replay* this trace each time an modular evaluation of the solution is needed. In our case this method (as implemented in RATRACER) improves the evaluation times of the IBP solution by a factor of ~10 compared to KIRA+FIREFLY. A further reduction by a factor of ~3 is achieved if the trace is *expanded in ε*, so that instead of outputting IBP coefficients as rational functions of ε, the output would be the terms of ε expansion of the IBP coefficients directly (this is also a builtin capability of RATRACER).

Because we perform IBP reduction for each phase-space point separately (setting all the kinematic variables to rational numbers) and combine it with ε expansion of the trace (eliminating ε as a variable), the outputs of the trace are no longer rational functions, but rather rational numbers. This means that we do not need to perform rational function reconstruction; we only need the Chinese remainder theorem and rational number reconstruction—much simpler and faster algorithms (which RATRACER implements).

Overall we can perform IBP reduction in under 2 minutes per phase-space point on 1 CPU core. We consider this to be fast enough for our needs.

2.3 Evaluating Feynman integrals with pySecDec

Once IBP reduction is complete we are left with evaluating the master integrals. For this we use the method of sector decomposition [41–44] as implemented in pySecDec [45–48]. We specifically rely on its ability to adaptively evaluate weighted sums of integrals. While in our case the 831 master integrals are split into 18000 sectors, each having multiple orders in ε, for a total of 28000 integrals, not all of these integrals contribute equally to the 9 symbolic structures we are interested in: some of them are naturally smaller or converge faster than the others, and others have small coefficients in front of them—pySecDec is equipped to automatically take this into account and sample the integrals that contribute the most, not wasting time on the others.

The adaptive sampling combined with the latest performance improvements in the form of the Disteval evaluator in version 1.6 allow us to calculate the value of the amplitudes with 0.3% precision in 5 minutes on a single NVidia A100 GPU for phase-space points in the bulk. For points closer to the edges of the phase-space, such as the high-energy region, the runtime grows the closer one gets to the edge—and does so indefinitely. The reason is numerical: when the kinematics becomes extreme a lot more of cancellations inside the integrals as well as between them happens, so each integral needs to be calculated to higher precision to achieve the overall precision target of the amplitude.

In fact, we have observed that for some points in the high-energy region the IBP coefficients grow very large, while the amplitude remains small, e.g.:

$$C = 10^{29} \quad + 10^{29} \quad + 10^{24} \quad + 10^{24} \quad + 10^{24} \quad$$
$$+ 10^{19} \quad + 10^{19} \quad + 10^{18} \quad + \cdots \approx 10^{-3}, \tag{7}$$
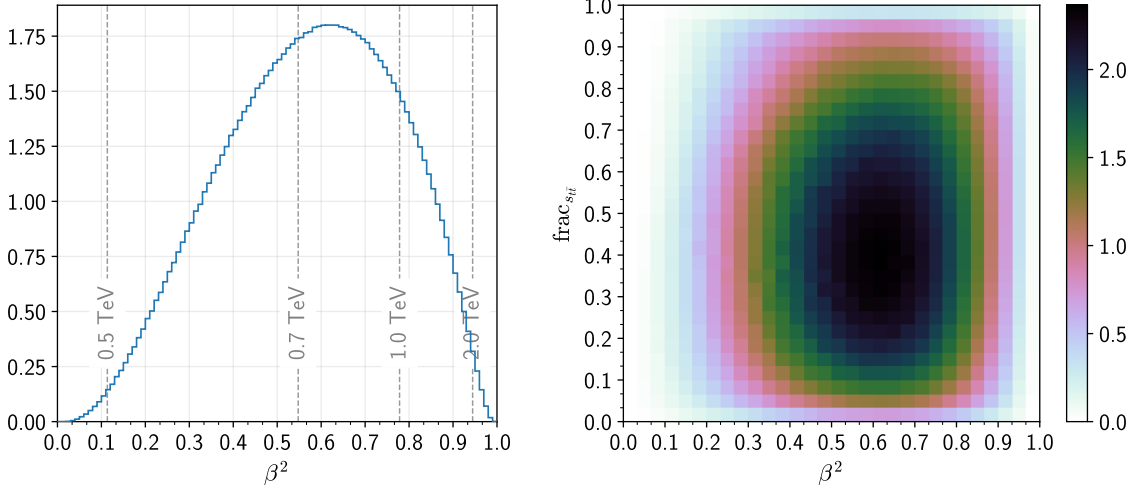
Figure 2: Event probability distribution in β^2 (left), and β^2 and $\text{frac}_{s_{t\bar{t}}}$ (right), according to the leading order $q\bar{q} \to t\bar{t}H$ amplitude. For this plot we take the energy of incoming quarks to be distributed according to the ABMP16 parton distribution functions [51] (which we evaluate via LHAPDF [52]), with the collision energy set to 13.6 TeV. We have also applied cuts on the top quark momenta in line with those reported in [1, 5]: we enforce a minimal transverse momentum of 25 GeV, a maximal rapidity of 4.5, and a separation ΔR in rapidity and azimuthal angle between the top quarks of $\Delta R > 0.4$.

meaning that there are more than 20 digits of numerical cancellation occurring. This means that even if we knew the values of each of the integral involved in the cancellation to the full machine double floating point precision, which is 16 digits, that would still be insufficient to get even a single significant digit of the amplitude. As a solution we have found that if we upgrade pySecDec to, instead of using *double*, use *double-double* [49, 50], a data type supporting up to 32 digits of precision, then it can in fact give more than 20 digits of precision to the integrals we need, and the giant cancellation is resolved. To this end, we use a custom implementation of double-double arithmetic, specifically written for use on the GPU.[1]

Note that getting 20 digits of precision for these integrals would not have been feasible with a Monte Carlo integrator. The reason why pySecDec is able to handle these integrals to such a high precision is the use of quasi-Monte Carlo integration [45, 47].

Seeing the performance degradation in the high-energy region, an important question is: is the phase-space region that numerical evaluation can effectively cover sufficient for phenomenological applications? The answer turns out to be *yes*: performing just the leading-order analysis, from Figure 2 we can see that 99% of the events happening at LHC are expected to lie within the incoming energy range of $[0.5; 2.1]$ TeV; in this region the pySecDec evaluation time can go up to 24 hours at 2.1 TeV, but quickly drops to 5 minutes at lower energies.

---

[1]On the CPU one would normally consider using quadruple precision floating point numbers for this task; these support up to 34 digits of precision. We chose otherwise because double-double is generally faster than quadruple, and because NVidia C compiler does not support either on the GPU, so a custom implementation is needed in any case.
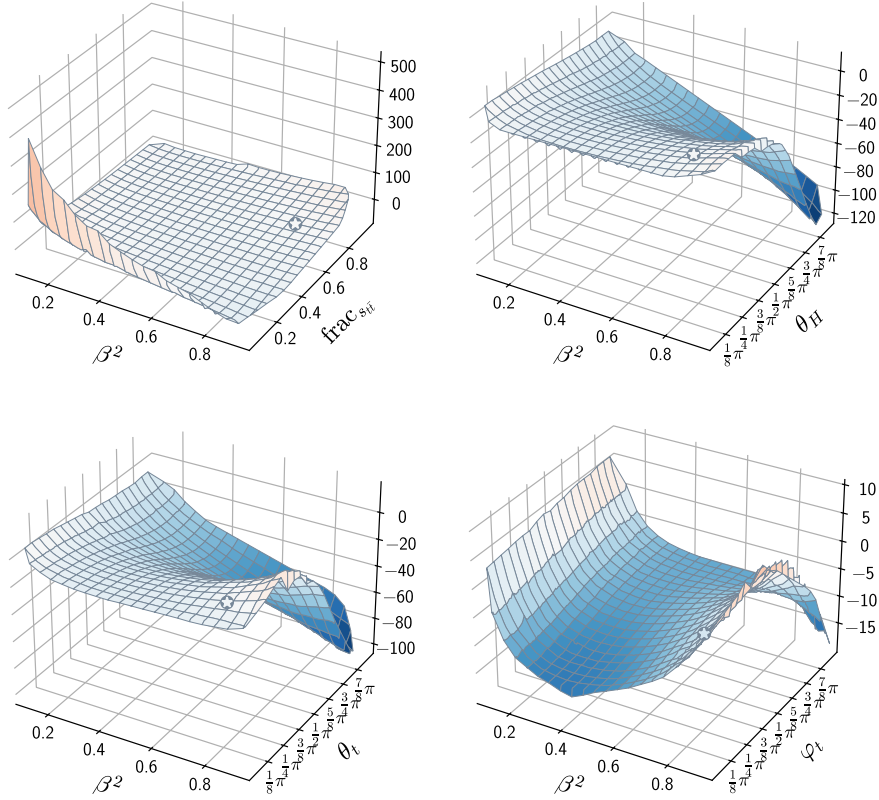
Figure 3: Two-dimensional slices of $C/\mathcal{A}$ around the center point eq. (8). The center point is marked with a star. For these plots we have set m_H^2 to $12/23\,m_t^2$, and the renormalization scale to $s/2$.

3. Results

To showcase the results we choose a center point of

$$\beta^2 = 0.8, \quad \text{frac}_{s_{t\bar{t}}} = 0.7, \quad \cos\theta_H = 0.8, \quad \cos\theta_t = 0.9, \quad \cos\varphi_t = 0.7, \tag{8}$$

and plot the calculated amplitudes in two-dimensional slices around it: see Figure 3 for the plots of two-loop amplitude C, and Figure 4 for equivalent one-loop results (as a reference for comparison). Note that the ratio $C/\mathcal{A}$ diverges close to the edge of $\text{frac}_{s_{t\bar{t}}} \to 0$ (same as $\mathcal{B}/\mathcal{A}$). This is a Coulomb singularity related to the exchange of a gluon between the outgoing top quarks This divergence is proportional to $1/\sqrt{\text{frac}_{s_{t\bar{t}}}}$ (see [53, Section 2.4.1]); it is suppressed by the phase-space density, which is $\propto \sqrt{\text{frac}_{s_{t\bar{t}}}}$ in this limit.

4. Summary and outlook

We have presented the calculation of the N_f part of the two-loop virtual amplitude for $q\bar{q} \to t\bar{t}H$ production. This calculation serves as a proof of concept of the overall method: using Rational Tracer for IBP reduction separately for each phase-space point, and a version of pySECDEC extended with support for double-double integration for evaluating the IBP-reduced amplitudes. We expect
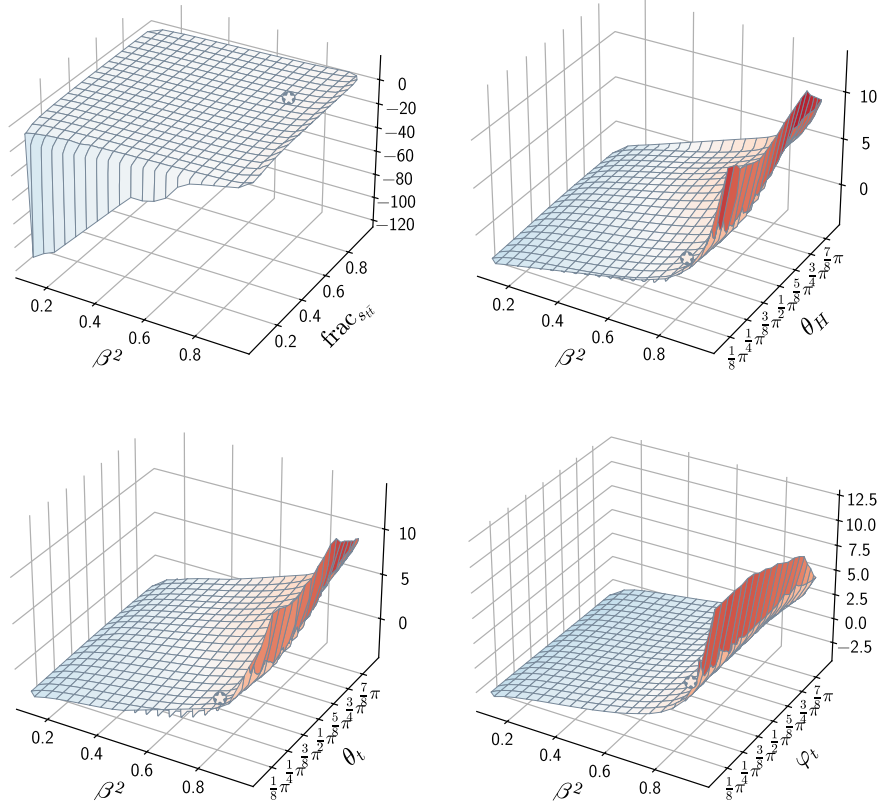
Figure 4: Same plots as in Figure 3, but for the one-loop amplitude $\mathcal{B}$.

to be able to apply this method to the calculation of the non-N_f parts of $q\bar{q} \to t\bar{t}H$, as well as to $gg \to t\bar{t}H$, thus opening the way towards full NNLO analysis of $t\bar{t}H$ production at LHC.

The main obstacle we see in such application is performance: practical use of the obtained results requires dense enough sampling of the relevant parts of the phase space, which translates into a high number of evaluations, due to the phase space being 5-dimensional, and possibly a large computational investment, because each phase-space point takes at least 5 minutes to evaluate. To alleviate these difficulties we would like to supplement the evaluated values with an interpolation framework, which should provide values of the amplitude across the relevant parts of the phase space with sufficient precision. Our experience shows that different interpolation methods might require different number of evaluations before the target precision is reached across the whole phase space, so selecting an appropriate interpolation framework is an open question that we see as an important part of the overall performance optimization.

Acknowledgements

References

[1] ATLAS collaboration, *Observation of Higgs boson production in association with a top quark pair at the LHC with the ATLAS detector*, *Phys. Lett. B* **784** (2018) 173 [1806.00425].

[2] CMS collaboration, *Observation of t$\bar{t}$H production*, *Phys. Rev. Lett.* **120** (2018) 231801 [1804.02610].

[3] ATLAS collaboration, *Evidence for the associated production of the Higgs boson and a top quark pair with the ATLAS detector*, *Phys. Rev. D* **97** (2018) 072003 [1712.08891].

[4] ATLAS collaboration, *Search for the standard model Higgs boson produced in association with top quarks and decaying into a b$\bar{b}$ pair in pp collisions at $\sqrt{s}$ = 13 TeV with the ATLAS detector*, *Phys. Rev. D* **97** (2018) 072016 [1712.08895].

[5] CMS collaboration, *Evidence for associated production of a Higgs boson with a top quark pair in final states with electrons, muons, and hadronically decaying τ leptons at $\sqrt{s}$ = 13 TeV*, *JHEP* **08** (2018) 066 [1803.05485].

[6] ATLAS collaboration, *CP Properties of Higgs Boson Interactions with Top Quarks in the t$\bar{t}$H and tH Processes Using $H \to \gamma\gamma$ with the ATLAS Detector*, *Phys. Rev. Lett.* **125** (2020) 061802 [2004.04545].

[7] ATLAS collaboration, *Probing the CP nature of the top–Higgs Yukawa coupling in t$\bar{t}$H and tH events with $H \to b\bar{b}$ decays using the ATLAS detector at the LHC*, *Phys. Lett. B* **849** (2024) 138469 [2303.05974].

[8] CMS collaboration, *Measurements of t$\bar{t}$H production and the CP structure of the Yukawa interaction between the Higgs boson and top quark in the diphoton decay channel*, *Phys. Rev. Lett.* **125** (2020) 061801 [2003.10866].

[9] CMS collaboration, *Measurement of the Higgs boson production rate in association with top quarks in final states with electrons, muons, and hadronically decaying tau leptons at $\sqrt{s}$ = 13 TeV*, *Eur. Phys. J. C* **81** (2021) 378 [2011.03652].

[10] CMS collaboration, *Search for CP violation in ttH and tH production in multilepton channels in proton-proton collisions at $\sqrt{s}$ = 13 TeV*, *JHEP* **07** (2023) 092 [2208.02686].

[11] P. Azzi et al., *Report from Working Group 1: Standard Model Physics at the HL-LHC and HE-LHC*, *CERN Yellow Rep. Monogr.* **7** (2019) 1 [1902.04070].

[12] A. Huss, J. Huston, S. Jones and M. Pellen, *Les Houches 2021—physics at TeV colliders: report on the standard model precision wishlist*, *J. Phys. G* **50** (2023) 043001 [2207.02122].

[13] ATLAS collaboration, *Snowmass White Paper Contribution: Physics with the Phase-2 ATLAS and CMS Detectors*, https://cds.cern.ch/record/2805993.

[14] S. Catani, I. Fabre, M. Grazzini and S. Kallweit, *t$\bar{t}$H production at NNLO: the flavour off-diagonal channels*, *Eur. Phys. J. C* **81** (2021) 491 [2102.03256].

PoS(LL2024)082

[15] S. Catani, S. Devoto, M. Grazzini, S. Kallweit, J. Mazzitelli and C. Savoini, *Higgs Boson Production in Association with a Top-Antitop Quark Pair in Next-to-Next-to-Leading Order QCD*, *Phys. Rev. Lett.* **130** (2023) 111902 [2210.07846].

[16] J. Chen, C. Ma, G. Wang, L.L. Yang and X. Ye, *Two-loop infrared singularities in the production of a Higgs boson associated with a top-quark pair*, *JHEP* **04** (2022) 025 [2202.02913].

[17] F. Febres Cordero, G. Figueiredo, M. Kraus, B. Page and L. Reina, *Two-Loop Master Integrals for Leading-Color $pp \to t\bar{t}H$ Amplitudes with a Light-Quark Loop*, 2312.08131.

[18] G. Wang, T. Xia, L.L. Yang and X. Ye, *Two-loop QCD amplitudes for $t\bar{t}H$ production from boosted limit*, 2402.00431.

[19] B. Agarwal, G. Heinrich, S.P. Jones, M. Kerner, S.Y. Klein, J. Lang, V. Magerya and A. Olsson, *Two-loop amplitudes for $t\bar{t}H$ production: the quark-initiated N_f-part*, *JHEP* **05** (2024) 013 [2402.03301].

[20] P. Nogueira, *Automatic Feynman Graph Generation*, *J. Comput. Phys.* **105** (1993) 279.

[21] V. Magerya, "Amplitude library (ALIBRARY): gluing all the tools needed for computing multi-loop amplitudes in QCD and beyond." https://github.com/magv/alibrary.

[22] B. Ruijl, T. Ueda and J. Vermaseren, *FORM version 4.2*, 1707.06453.

[23] T. van Ritbergen, A.N. Schellekens and J.A.M. Vermaseren, *Group theory factors for Feynman diagrams*, *Int. J. Mod. Phys. A* **14** (1999) 41 [hep-ph/9802376].

[24] V. Magerya, *Semi- and Fully-Inclusive Phase-Space Integrals at Four Loops*, Ph.D. thesis, Hamburg U., 7, 2022. https://ediss.sub.uni-hamburg.de/handle/ediss/9787.

[25] P. Maierhöfer, J. Usovitsch and P. Uwer, *Kira—A Feynman integral reduction program*, *Comput. Phys. Commun.* **230** (2018) 99 [1705.05610].

[26] J. Klappert, F. Lange, P. Maierhöfer and J. Usovitsch, *Integral reduction with Kira 2.0 and finite field methods*, *Comput. Phys. Commun.* **266** (2021) 108024 [2008.06494].

[27] V. Magerya, RATIONAL TRACER: *a Tool for Faster Rational Function Reconstruction*, 2211.03572, https://github.com/magv/ratracer.

[28] A. Ferroglia, M. Neubert, B.D. Pecjak and L.L. Yang, *Two-loop divergences of massive scattering amplitudes in non-abelian gauge theories*, *JHEP* **11** (2009) 062 [0908.3676].

[29] P. Bärnreuther, M. Czakon and P. Fiedler, *Virtual amplitudes and threshold behaviour of hadronic top-quark pair-production cross sections*, *JHEP* **02** (2014) 078 [1312.6279].

[30] A. von Manteuffel, E. Panzer and R.M. Schabinger, *A quasi-finite basis for multi-loop Feynman integrals*, *JHEP* **02** (2015) 120 [1411.7392].

[31] A.V. Smirnov and V.A. Smirnov, *How to choose master integrals*, *Nucl. Phys. B* **960** (2020) 115213 [2002.08042].

[32] J. Usovitsch, *Factorization of denominators in integration-by-parts reductions*, 2002.08173.

[33] S. Laporta, *High-precision calculation of multiloop Feynman integrals by difference equations*, *Int. J. Mod. Phys. A* **15** (2000) 5087 [hep-ph/0102033].

[34] A. von Manteuffel and R.M. Schabinger, *A novel approach to integration by parts reduction*, *Phys. Lett. B* **744** (2015) 101 [1406.4513].

[35] T. Peraro, *Scattering amplitudes over finite fields and multivariate functional reconstruction*, *JHEP* **12** (2016) 030 [1608.01902].

[36] J. Klappert and F. Lange, *Reconstructing rational functions with FireFly*, *Comput. Phys. Commun.* **247** (2020) 106951 [1904.00009].

[37] J. Klappert, S.Y. Klein and F. Lange, *Interpolation of dense and sparse rational functions and other improvements in FireFly*, *Comput. Phys. Commun.* **264** (2021) 107968 [2004.01463].

[38] A.V. Smirnov and F.S. Chuharev, *FIRE6: Feynman Integral REduction with Modular Arithmetic*, *Comput. Phys. Commun.* **247** (2020) 106877 [1901.07808].

[39] T. Peraro, *FiniteFlow: multivariate functional reconstruction using finite fields and dataflow graphs*, *JHEP* **07** (2019) 031 [1905.08019].

[40] S. Abreu, J. Dormans, F. Febres Cordero, H. Ita, M. Kraus, B. Page, E. Pascual, M.S. Ruf and V. Sotnikov, *Caravel: A C++ framework for the computation of multi-loop amplitudes with numerical unitarity*, *Comput. Phys. Commun.* **267** (2021) 108069 [2009.11957].

[41] K. Hepp, *Proof of the Bogolyubov–Parasiuk theorem on renormalization*, *Commun. Math. Phys.* **2** (1966) 301.

[42] M. Roth and A. Denner, *High-energy approximation of one loop Feynman integrals*, *Nucl. Phys. B* **479** (1996) 495 [hep-ph/9605420].

[43] T. Binoth and G. Heinrich, *An automatized algorithm to compute infrared divergent multiloop integrals*, *Nucl. Phys. B* **585** (2000) 741 [hep-ph/0004013].

[44] G. Heinrich, *Sector Decomposition*, *Int. J. Mod. Phys. A* **23** (2008) 1457 [0803.4177].

[45] G. Heinrich, S.P. Jones, M. Kerner, V. Magerya, A. Olsson and J. Schlenk, *Numerical scattering amplitudes with pySecDec*, *Comput. Phys. Commun.* **295** (2024) 108956 [2305.19768].

[46] G. Heinrich, S. Jahn, S.P. Jones, M. Kerner, F. Langer, V. Magerya, A. Pöldaru, J. Schlenk and E. Villa, *Expansion by regions with pySecDec*, *Comput. Phys. Commun.* **273** (2022) 108267 [2108.10807].

[47] S. Borowka, G. Heinrich, S. Jahn, S.P. Jones, M. Kerner and J. Schlenk, *A GPU compatible quasi-Monte Carlo integrator interfaced to pySecDec*, *Comput. Phys. Commun.* **240** (2019) 120 [1811.11720].

[48] S. Borowka, G. Heinrich, S. Jahn, S.P. Jones, M. Kerner, J. Schlenk and T. Zirke, *pySecDec: a toolbox for the numerical evaluation of multi-scale integrals*, *Comput. Phys. Commun.* **222** (2018) 313 [1703.09692].

[49] D.H. Bailey, X.S. Li and Y. Hida, *QD: A Double-Double/Quad-Double Package*, 6, 2003. 10.11578/dc.20210416.14, https://www.davidhbailey.com/dhbsoftware/.

[50] R.J. Shewchuk, *Adaptive Precision Floating-Point Arithmetic and Fast Robust Geometric Predicates*, *Discrete Comput. Geom.* **18** (1997) 305.

[51] S. Alekhin, J. Blümlein, S. Moch and R. Placakyte, *Parton distribution functions, α_s, and heavy-quark masses for LHC Run II*, *Phys. Rev. D* **96** (2017) 014011 [1701.05838].

[52] A. Buckley, J. Ferrando, S. Lloyd, K. Nordström, B. Page, M. Rüfenacht, M. Schönherr and G. Watt, *LHAPDF6: parton density access in the LHC precision era*, *Eur. Phys. J. C* **75** (2015) 132 [1412.7420].

[53] W. Beenakker, S. Dittmaier, M. Krämer, B. Plümper, M. Spira and P. Zerwas, *NLO QCD corrections to $t\bar{t}H$ production in hadron collisions*, *Nucl. Phys. B* **653** (2003) 151 [hep-ph/0211352].